Journal of Alloys and Compounds 480 (2009) 270–274

Contents lists available at ScienceDirect

Journal of Alloys and Compounds

journal homepage: www.elsevier.com/locate/jallcom

Bimetallic nanoalloys: Preparation, characterization and their catalytic activity☆

Gurdip Singh*, I.P.S. Kapoor, Shalini Dubey

Chemistry Department, D.D.U. Gorakhpur University, Gorakhpur 273009, India

ARTICLE INFO

Article history:
Received 6 December 2008
Received in revised form 3 February 2009
Accepted 8 February 2009
Available online 20 February 2009

Keywords:
Bimetallic nanoalloys
Ammonium perchlorate
Thermal decomposition
Ignition delay
Burning rate
Composite solid propellant

ABSTRACT

Bimetallic nanoalloys (BMNAs) of 3d-series (Ni–Cu, Ni–Co and Ni–Zn) were prepared by hydrazine reduction of respective metal chloride in ethylene glycol at 60 °C. These were characterized by X-ray diffraction (XRD) and transmission electron microscopy (TEM) and particle size was found to be in the order of 34, 43 and 30 nm, respectively. The thermolysis of ammonium perchlorate (AP) and AP-HTPB composite solid propellants was found to be catalyzed with BMNAs and burning rate was found to be enhanced considerably. TG and ignition delay studies demonstrated that higher temperature decomposition (HTD) of AP is enhanced enormously by these additives and Ni–Co nanoalloy is the best catalyst.

1. Introduction

Ammonium perchlorate (AP) is most important oxidizer for composite solid propellants (CSPs) [1]. The characteristic of the thermal decomposition of AP are believed to influence the performance of CSPs and are remarkably sensitive to additives [2–7]. The burning rate of CSPs having AP in the matrix of polymeric fuel can be accelerated by the addition of small amount of transition metal oxides. Most recently, new catalyst of nano size have been reported which are more active than commonly used one.

In material science, the range of properties of metallic systems can be greatly extended by taking mixtures of elements to generate intermetallic compounds and alloys [8]. The rich diversity of compositions, structures and properties of metallic alloys has led to widespread applications in electronic and catalysis. To fabricate materials with well defined, controllable properties and structures on the nanometer scale, afforded by intermetallic materials have generated interest in bimetallic nanoalloys. Surface structures, composition and segregation properties of nanoalloys are of interest as they are important in determining chemical reactivity especially the catalytic activity. Moreover, nanoalloys are also of interest as they may display structures and properties which are distinct from those of the pure elemental cluster and bulk alloys. Nanoallloys have been prepared by low temperature synthetic pathway, co-decomposition, co-reduction methods, etc. [8].

In the present work, bimetallic nanoalloys (BMNAs) were prepared by hydrazine reduction of metal chloride in ethylene glycol without use of any protective agent [9]. The particle size of the nanoalloys was evaluated. Further a comprehensive investigation on thermolysis of AP and AP-HTPB with and without catalyst have been undertaken using TG, ignition delay and burning rate studies.

2. Experimental

2.1. Materials

AP obtained from CECRI, Karaikudi was used without further purification. $NiCl_2$ (Qualigens), $CoCl_2$ (Analytical Rasayan), $CuCl_2$ (Merck), $ZnCl_2$ (Merck) HTPB (VSSC, Thiruvanthapuram), IPDI (Merck) and DOA (Merck) were used as received.

2.2. Preparation of BMNAs

All BMNAs were prepared by hydrazine reduction in ethylene glycol as reported earlier [9]. An appropriate amount of metal chloride (1.25 mM) was dissolved directly in ethylene glycol followed by addition of an appropriate amount of hydrazine (0.05–0.9 M) and of 1.0 M NaOH solution (10–72 μl). At 60 °C, metal nanoalloys were formed after about 1 h, in a capped bottle with stirring. The reaction was performed in an organic solvent instead of aqueous solution, so it was relatively easy to form nanoalloys. Nitrogen gas was produced and bubbled up continuously during reaction which created an inert atmosphere.

2.3. Characterization

X-ray diffraction (XRD) measurement were performed on the BMNAs by an X-ray diffractometer using Cu Kα radiation (λ = 1.5418) and diffraction pattern is shown in Fig. 1. Crystallite size was determined according to the half width of the highest intensity diffraction peak using Debye–Scherrer's equation [10] (Table 1). The size and morphology of the BMNAs were also studied by transmission electron microscope (TEM) model No. CM200, operating voltage 20–200 kV and resolution 2.4 Å (Fig. 2).

☆ Part 70.

* Corresponding author. Tel.: +91 551 2200745(R)/2202856(O); fax: +91 551 2340459.
E-mail address: gsingh4us@yahoo.com (G. Singh).

0925-8388/$ – see front matter © 2009 Elsevier B.V. All rights reserved.
doi:10.1016/j.jallcom.2009.02.024

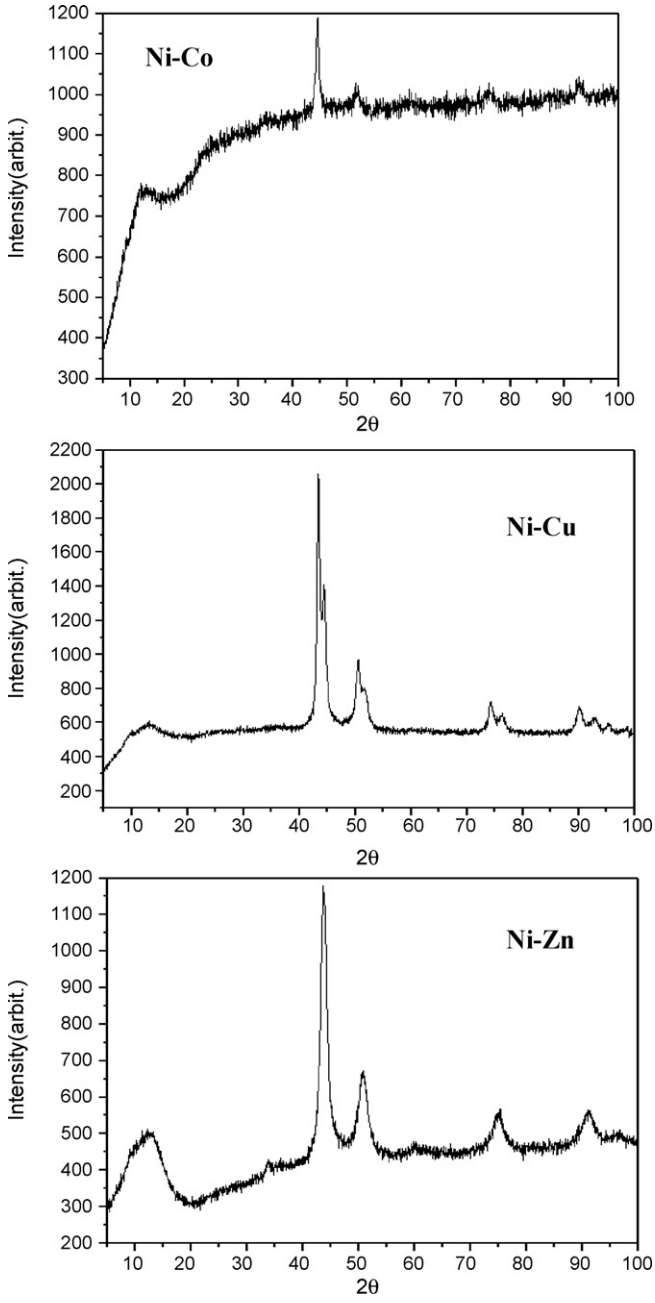

Fig. 1. XRD patterns.

Table 1
Crystal size of BMNAs.

Nanoalloy	Particle size (nm)	
	XRD	TEM
Ni–Co	37.3	43
Ni–Cu	26.5	34
Ni–Zn	30.1	30

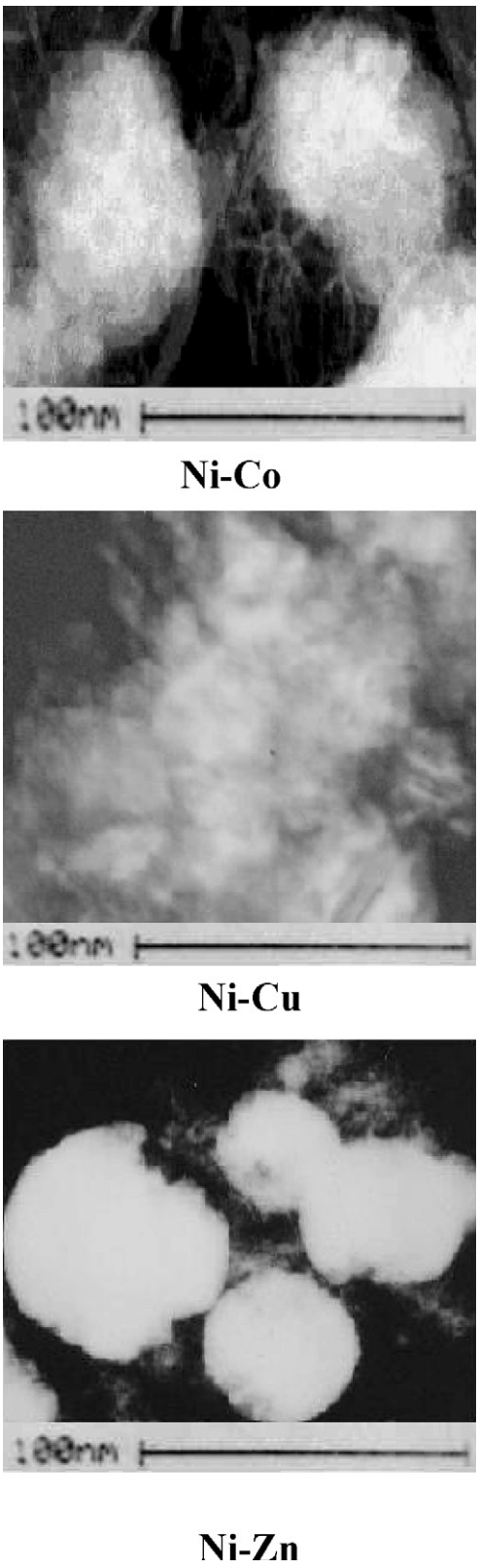

Fig. 2. TEM images.

3. Thermolysis of AP in presence of BMNAs

3.1. Simultaneous TG-DTG-DSC

TG-DSC-DTG thermogram (Fig. 3) on pure AP and AP with BMNAs (by mixing in ratio of 99:1) were recorded on the samples (~12 mg) using Perkin Elmer (Pyris Diamond) under nitrogen atmosphere (200 ml/min) at a heating rate 10 °C/min

3.2. Isothermal TG

Isothermal TG on the AP with and without BMNAs by varying compositions (0.25, 0.5, 1 and 2% by mass) at 300 °C under static air atmosphere were recorded using indigenously fabricated TG [11] apparatus (Fig. 4).

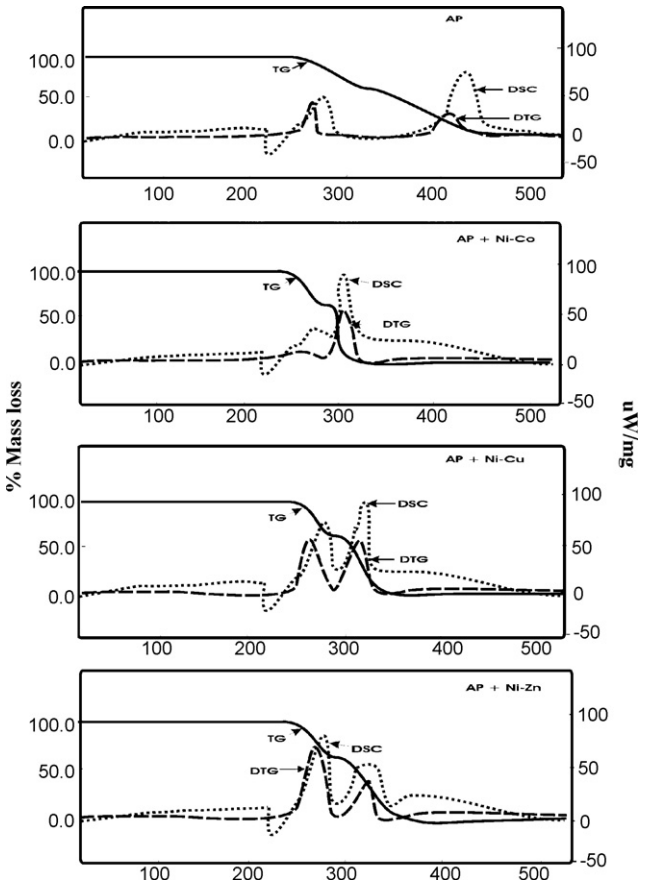

Fig. 3. TG-DTG-DSC thermogram.

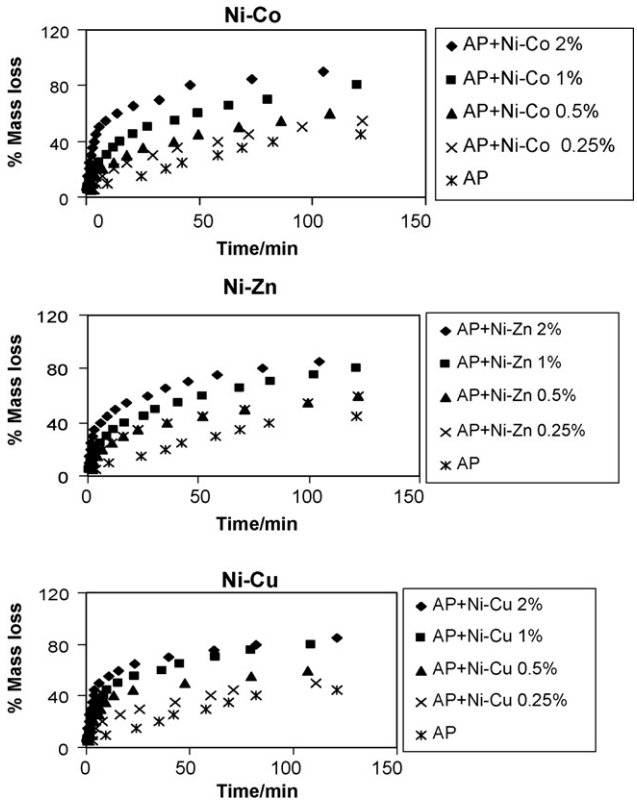

Fig. 4. Isothermal TG of various % of BMNAs in AP at 300 °C.

3.3. Ignition delay (D_i) measurments

This measurement was undertaken using the tube furnace (TF) technique [12] in the temperature range of 360–420 °C. Twenty milligrams of samples (AP and AP with BMNAs in same ratio as in TG) were taken in an ignition tube and time interval determined with help of stop watch, between the insertion of the ignition tube into the TF and the moment of ignition indicated by the appearance of fumes with light, gave the value of ignition delay in seconds. The sample was inserted into the TF with the help of a bent wire. The time for the insertion of the ignition tube into the TF was kept constant throughout each run. The accuracy of temperature measurements of TF was ±1 °C. Each run was taken five times and mean D_i value are reported in Table 2. The D_i data were found to fit in the Eq. (1) [13–15].

$$D_i = A \exp\left(\frac{E_a}{RT}\right) \quad (1)$$

where, E_a is activation energy for thermal explosion. A is the pre-exponential factor, and T the absolute temperature. E_a's assessed by Eq. (1) along with the correlation coefficients (r) are given in Table 3.

Table 2
DTG and DSC phenomenological data of the AP and AP with BMNAs.

Samples	DTG		DSC	
	Peak (temperature (°C))	Nature	Peak (temperature (°C))	Nature
AP	282	Exo	285	Exo
	410	Exo	420	Exo
Ni–Co	267	Exo	275	Exo
	300	Exo	300	Exo
Ni–Cu	277	Exo	279	Exo
	324	Exo	325	Exo
Ni–Zn	290	Exo	280	Exo
	340	Exo	336	Exo

3.4. Preparation of CSPs

CSP samples were prepared by dry mixing [16] of AP [100–200 and 200–400 mesh (3:1)] with BMNAs (1% by wt.). The solid mate-

Table 3
Ignition delay (D_i), activation energy for ignition delay (E_a) and correlation coefficient of AP and AP + BMNAs (1% by wt.).

Sample	D_i (s)					E_a (kJ/mol)	r (Correlation coefficient)	$-\ln A$
	360 ± 1 °C	375 ± 1 °C	390 ± 1 °C	405 ± 1 °C	420 ± 1 °C			
AP	105	93	85	71	60	49.14	0.9897	4.65
AP + Ni–Co (1% wt.)	64	59	53	48	45	22.18	0.9977	0.04
AP + Ni–Cu (1% wt.)	75	68	64	55	48	26.78	0.9849	0.75
AP + Ni–Zn (1% wt.)	90	85	75	63	55	31.13	0.9834	1.37

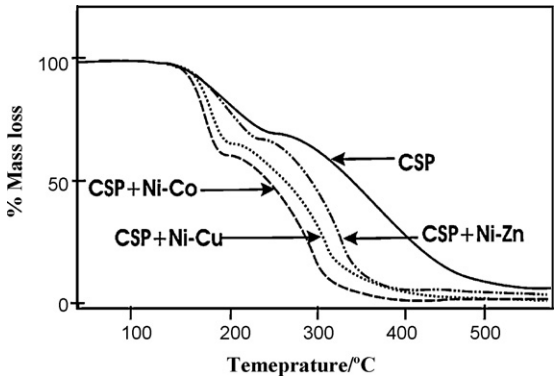

Fig. 5. TG thermogram of CSPs with and without BTMNs.

rials were mixed with HTPB in the ratio of 3:1. The binder part includes the curing agent (IPDI) in equivalent ratio to HTPB and plasticizer (DOA, 30% to HTPB). During mixing of the solid components with HTPB, temperature was maintained at 60 °C for 1 h. The propellants were prepared with and without BMNAs, casted into aluminum plates having dimensions 1 cm × 3 cm × 10 cm. The samples were cured in an incubator at 70 °C for 8–10 days [17].

3.5. Measurement of burning rate

The cured propellant samples were cut into smaller pieces having dimensions 0.8 cm × 0.8 cm × 9.0 cm and burning rate was measured at ambient pressure by fuse wire technique [17]. An average of 3 measurements was taken which are within experimental error and results are reported in Table 3.

3.6. Thermal decomposition of CSPs

The non-isothermal decomposition of propellants with and without BMNA were carried out in static air using indigenously fabricated TG apparatus at a heating rate of 10 °C/min taking 20 mg of samples. The plots of percent decomposition vs. temperature are given in Fig. 5 and ignition delay measurements were done as reported earlier and data shown in Table 5.

4. Results and discussion

BMNAs are prepared by hydrazine reduction in ethylene glycol, which is better than earlier reported method [9]. There is no need of any protective agent which is difficult to remove completely from the metal surface by simple washing. The XRD patterns (Fig. 1) for all these BMNAs show considerable broadening of the peaks, which are due to the presence of very small crystallites.

Table 4
Burning rate of CSPs with and without BMNAs (1% by wt.).

Sample	Burning rate (mm/s)	r^*/r
CSP	1.22	1.00
CSP + Ni–Co	2.08	1.71
CSP + Ni–Cu	1.77	1.45
CSP + Ni–Zn	1.59	1.30

r^* and r are burning rate of CSP with and without BMNA, respectively.

TEM images are in range of 43–30 nm, which is in good agreement with that estimated by Scherrer equation from the XRD pattern. Average size for BMNAs are shown in Table 1.

The non-isothermal TG thermogram in flowing N_2 atmosphere (Fig. 3) clearly indicates that thermal decomposition of AP takes place in two steps [18–20]. TG thermogram (Fig. 3) for AP with BMNAs does confirm that nanocrystals affect both LTD and HTD of AP, addition of catalyst, not only increases the mass loss of AP but also lower the HTD range of AP to form gaseous products. DTG also confirms lowering temperature of HTD (Table 2).

DSC thermogram (Fig. 3) for the decomposition of pure AP shows three events. The endothermic peak at 237 °C represents the transition of AP from orthorhombic to cubic form [1]. The first step is an exothermic peak observed at 285 °C corresponds to LTD process and second peak corresponding to HTD process observed at 420 °C. DSC thermogram of AP in presence of BMNAs shows noticeable change (shifting to lower temperature) in the decomposition pattern.

The effect of BMNAs on thermolysis of AP by varying their amount (Fig. 4), experimental results clearly indicate that the catalytic activity increases with increasing amount of the BMNAs in AP. AP with BMNAs ignited with noise at sudden high temperature. Computational calculation shows that activation energy for ignition for AP is lowered by the BMNAs (Table 3). Results reported in table clearly shows that BMNAs enhance the burning rate '*r*' of CSPs which is highest for Ni–Co near about two times and lowest for Ni–Zn nanoalloy (Table 4).

Most of the studies suggested that ballistic modifiers are active mainly in the condense phase at AP-binder interface [21]. TG thermograms shown in Fig. 5 indicates that the condensed phase reactions are occurring in CSPs. CSPs has two step decomposition namely LTD and HTD whereas in case of propellants with BMNAs, the thermal decomposition occurs at much lower temperature in case of HTD, which may be due to the activity of BMNAs (Fig. 5). Ignition delay and their kinetic parameters are shown in Table 5

CSPs also ignited with noise and flame at sudden high temperature. Computational calculation shows that activation energy for ignition of CSPs lowered by the BMNAs. Summarizing these results, it may be inferred that BMNA can be used as catalyst for AP and CSPs.

Table 5
Ignition delay (D_i), activation energy for ignition delay (E_a) and correlation coefficient of CSPs with and without BMNAs (1% by wt.).

Sample	D_i (s)					E_a (kJ/mol)	r (Correlation coefficient)	$-\ln A$
	360 ± 1 °C	375 ± 1 °C	390 ± 1 °C	405 ± 1 °C	420 ± 1 °C			
CSP	68	62	55	52	49	20.3	0.9800	0.36
CSP + Ni–Co	54	50	46	44	41	16.5	0.9970	0.67
CSP + Ni–Cu	57	53	48	45	43	17.7	0.9843	0.85
CSP + Ni–Zn	62	56	50	48	46	18.4	0.9800	0.62

5. Conclusions

BMNAs were prepared by hydrazine reduction method and used as catalysts in the thermolysis of AP and CSPs. The burning rate was found to be enhanced with BMNAs. TG-DTG-DSC and ignition delay studies demonstrated that HTD of AP is enhancing enormously by these catalysts and Ni–Co nanoalloy was found to be the best.

Acknowledgments

The authors are grateful to Head, Chemistry Department of D.D.U. Gorakhpur University for laboratory facility, IIT Roorkee for XRD and TG-DTG-DSC studies and to IIT Bombay for TEM images. Thanks are also due to financial assistance by CSIR for providing Emeritus Scientist to G. Singh and UGC for UGC-DSA fellowship to Shalini Dubey.

References

[1] V.V. Boldyerv, Thermochim. Acta 443 (2006) 1–36.
[2] G. Singh, I.P.S. Kapoor, S. Dubey, P.F. Siril, J. Sci. Conf. Proc. 1 (2008) 7–14.
[3] G. Singh, I.P.S. Kapoor, S. Dubey, P.F. Siril, Propellants Explosives Pyrotechnics 34 (1) (2009) 72–77.
[4] J. Zhu, D. Li, H. Chen, X. Yang, L. Lu, X. Wang, Mater. Lett. 58 (2004) 3324–3327.
[5] L. Liu, F. Li, L. Tan, L. Miang, Y. Yi, Propellants Explosives and Pyrotechnics 1 (2004) 29.
[6] G. Singh, I.P.S. Kapoor, S. Dubey, P.F. Siril, J.H. Yi, F.Q. Zhao, R.-Z. Hu, Thermochim. Acta 477 (2008) 42–46.
[7] I.P.S. Kapoor, P. Srivastava G. Singh, Propellants, Explosives, Pyrotechnics, in press.
[8] R. Ferrando, J. Jellinek, R.L. Johnston, Chem. Rev. 108 (3) (2008) 845–910.
[9] S.-H. Wu, D.-H. Chen, J. Colloid Interface Sci. 59 (2003) 282–286.
[10] L.S. Birks, H. Friedman, J. Appl. Phys. 17 (1946) 687.
[11] G. Singh, R.R. Singh, Res. Ind. 23 (1978) 92.
[12] G. Singh, I.P.S. Kapoor, S.K. Vasudeva, Indian J. Technol. 24 (1991) 589.
[13] N. Semonov, Chemical Kinetics and chain reaction, Clarendon Press, Oxford, U.K., 1935, Chapter 18.
[14] E.S. Freeman, S. Gordon, J. Phys. Chem. 956 (1960) 867.
[15] J. Zinn, R.N. Rogers, J. Phys. Chem. 66 (1962) 2646.
[16] S. Krishna, R.D. Swami, J. Propul. Power 13 (2) (1997) 207.
[17] G. Singh, S. Prem Felix, Combust. Flame 132 (2003) 422–432.
[18] L.L. Bircumshaw, B.H. Newmann, Proc. Roy. Soc. A 227 (1954) 115.
[19] P.M.W. Jacobs, G.S. Parasone, Combust. Flame 13 (1969) 419.
[20] W.A. Rosser, S.H. Inami, Combust. Flame 12 (1968) 427.
[21] S.R. Chakravarthy, E.W. Price, R.K. Sigman, J. Propul. Power 13 (4) (1997) 471.